Exploring the Picosecond Time Domain of the Solvation Dynamics of Coumarin 153 within β-Cyclodextrins

Javier Rodriguez,[†] Jordi Martí,[‡] Elvira Guàrdia,[‡] and Daniel Laria*,[†]

Departamento de Física, Comisión Nacional de Energia Atómica, Avenida Libertador 8250, 1429, Buenos Aires, Argentina, Departamento de Química Inorgánica, Analítica y Química-Física e INQUIMAE, Facultad de Ciencias Exactas y Naturales, Universidad de Buenos Aires, Ciudad Universitaria, Pabellón II, 1428, Buenos Aires, Argentina, and Departament de Fısica i Enginyeria Nuclear, Universitat Politecnica de Catalunya, B4-B5 Campus Nord 08034, Barcelona, Spain

Received: March 18, 2008; Revised Manuscript Received: April 25, 2008

Downloaded by COMISION NAC DE ENERGIA ATOMICA CNEA on October 7, 2009 | http://pubs.acs.org
Publication Date (Web): July 2, 2008 | doi: 10.1021/jp8023765

We report molecular dynamics simulation results of equilibrium and dynamical characteristics pertaining to the solvation of the dye coumarin 153 (C153) trapped within hydrophobic cavities of di- and trimethylated β-cyclodextrins (CD) in aqueous solutions. We found that stable configurations of the encapsulated probe are characterized by a slanted docking, in which the plane of the C153 lies mostly parallel to one of the glucose units of the CD. "In and out" dynamical modes of the encapsulated probe present very small amplitudes. The rotational dynamics of the trapped coumarin can be cast in terms of a simple model that includes diffusive motions within a local restrictive environment coupled to the overall rotational motion of the CD. We have examined the early stages of the solvation response of the environment following a vertical excitation of the probe. Regardless of the degree of CD methylation, the water dynamical response seems to be completed within 2−3 ps and does not differ substantially from that observed for nonencapsulated probes. The CD response is characterized by a single, subpicosecond relaxation that involves intramolecular motions. We also explored dynamical modes that could account for the recently reported persistence of Stokes shifts in the nanosecond time domain. In all cases, the only sources of ultraslow dynamics that we detected were those associated with gauche−trans interconversions in primary hydroxyl chains of the CD, which do not seem to be directly connected to the electronic excitation of the probe.

I. Introduction

Cyclodextrins (CD) represent versatile complexing agents with widespread applications in many areas of solution chemistry.[1] Perhaps the most remarkable characteristic exhibited by CD is their unusual ability to stabilize sparingly soluble organic molecules in aqueous phases. This distinctive feature derives from their molecular shape, usually portrayed in terms of an inner cylindrical hydrophobic cavity flanked by several glucose units, assembled through a sequence of α(1−4) glycosidic linkages. By a careful choice of cavity size and functionalization, it is possible to selectively control the type of trapped molecules and to modulate their chemical reactivity as well.[2–9]

In recent years, useful insights about the characteristics of the confinement prevailing within CD cavities have been obtained by a variety of experimental techniques. Without being exhaustive, the list includes electron spin resonance (ESR),[10] ^{1}H NMR,[11] ^{2}H and ^{13}C magnetic nuclear resonance,[12] and fluorescence spectroscopy.[13–21] The present work is largely motivated by results presented in a recent paper by Sen et al.[21] dealing with the anisotropy decay and solvation dynamics of coumarin 153 (C153) encapsulated within two CD of similar sizes, albeit different functionalization.

C153 is a popular laser dye that has been extensively used in steady-state and time-dependent fluorescence experiments to unveil microscopic details related to solvation phenomena in environments such as polar and nonpolar bulk liquid phases,[22,23] reverse micelles,[24] ionic liquids,[25,26] protein−surfactant complexes,[27] supercritical fluids,[28] and confined polar liquids,[29] to cite a few important examples. One striking feature of the results reported by Sen et al.[21] concerns the appearance of ultraslow relaxation branches—on the order of a few nanoseconds—not observed in experiments performed on "free" (nonencapsulated) coumarin dyes in solution. Similar observations were reported more than 10 years ago by Vajda et al.,[17] who measured time-dependent Stokes shifts of two different coumarins (C480 and C460) within larger cyclodextrin cavities. Following the experiments by Vajda et al.,[17] Nandi and Bagchi[30] were able to rationalize important features of the observed solvation responses, using two analytical approaches based on continuum and molecular hydrodynamic theories. We remark that the overall retardation observed in these experiments is intimately related to a more general class of phenomena involving water confined within geometrically restrictive environments, a subject of primary interest in biological sciences.[31–33]

Our approach to tackle the problem has relied on the use of massive molecular dynamics experiments. As such, in the present work, two large and well-differentiated bodies of previous simulation experiments converge: on the one hand, those that have addressed the analysis of the solvation of CD in aqueous solutions,[34–45] and on the other hand, those in which equilibrium and dynamical characteristics of the solvation response in solution were examined.[46–54] Consideration of the complexities derived from the results of these previous studies anticipates a solvation scenario whose description will necessarily involve a large variety of relevant length scales and an

* Corresponding author.
[†] Comisión Nacional de Energia Atómica and Universidad de Buenos Aires.
[‡] Universitat Politecnica de Catalunya.

10.1021/jp8023765 CCC: $40.75 © 2008 American Chemical Society
Published on Web 07/02/2008

Downloaded by COMISION NAC DE ENERGIA ATOMICA CNEA on October 7, 2009 | http://pubs.acs.org
Publication Date (Web): July 2, 2008 | doi: 10.1021/jp8023765

equally diverse spectrum of characteristic times. As a consequence, we believe that the consideration of more simplified models based on, for example, spherical hydrophobic cavities or more simple model solutes,[55,56] although physically sound, may leave behind important aspects that cannot be disregarded when one analyzes the solvation of a polyatomic probe in a CD cavity.

Given the degree of molecular detail that we have incorporated in our simulation experiments, the present study represents an important step forward toward more realistic descriptions of the solvation of complex solutes in solution. Of course, such a level of microscopic detail restricted our ability to conduct simulation experiments over long enough time intervals that would allow us to clearly identify the microscopic origins of the modes that drive the ultraslow behavior of the responses. Yet, the results that we will present open new and insightful perspectives to rationalize direct experimental information. The organization of the paper is as follows: in section II we describe the model and the simulation procedure. Section III contains information about equilibrium solvation structures of confined probes. The dynamical results are presented in sections IV and V, where we describe results for the rotational dynamics and the solvation response. In section VI we present new insights about possible origins of the ultraslow dynamics reported in the experiments. A general discussion of the most relevant results of the paper is presented in section VII.

II. Model and Methods

The systems under investigation were composed of a CD−C153 complex immersed in a fully periodic, 30 Å × 30 Å × 30 Å box containing 880 water molecules. The solvent and the C153 were modeled as nonpolarizable, rigid bodies containing a collection of interaction sites. All intermolecular interactions consisted of a sum of Lennard-Jones plus Coulombic site−site contributions. Water molecules were modeled with the SPC model,[57] whereas for the C153 molecule we implemented the all-atom parametrization proposed by Martins and Skaf.[49] The fluorescent probe comprised a total of 36 sites, lying in a planar geometrical arrangement, with approximate linear dimensions 10 Å × 6 Å (see Figure 1a). To compute partial charges for the S_0 and S_1 states, Martins and Skaf resorted to ab initio calculations at the restricted Hartree−Fock level, with full geometry optimization with a 6-31G(d,p) basis set. A list of the partial charges for the ground and first excited electronic states of the probe can be obtained in Table 1 of ref 49, to which we refer the reader for additional details of the quantum calculations. The resulting dipole moments of the molecule are $\mu = 6.34$ and 10.7 D for the S_0 and S_1 states, respectively. These values agree reasonably well with the corresponding experimental results, 6.55 and 14.48 D; [58] in both cases, the dipole moments of the probe are approximately aligned along the $r_{C5}-r_{C10}$ vector (see also Figure 1a).

Two different CD molecules were investigated: The first one corresponded to the partially methylated heptakis(2,6-di-*O*-methyl)-β-cyclodextrin (DIMEB), while the second was the permethylated one, heptakis(2,3,6-tri-*O*-methyl)-β-cyclodextrin (TRIMEB). According to the united atom description for CH_2 and CH_3 groups, both molecules include 98 interaction sites (see Figure 1b). The initial coordinates of CD were obtained from X-ray information.[59] Length and energy parameters for inter- and intramolecular potentials corresponded to the GROMACS force field and were taken from ref 60. This parametrization has proved to yield very good agreement with experimental information for structural features of several CD.[61–63]

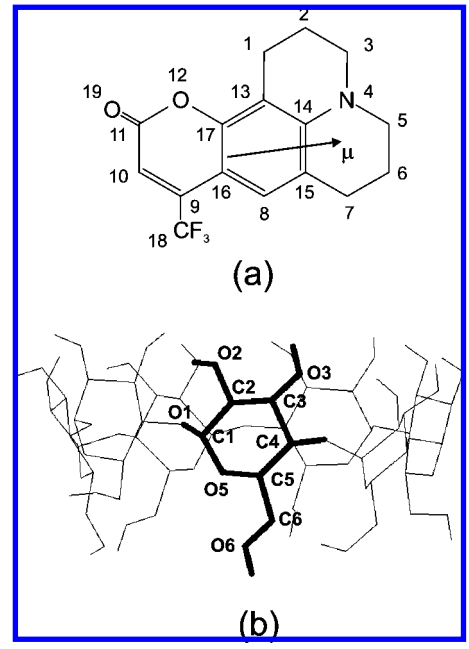

Figure 1. (a) Coumarin 153. (b) Molecular geometry and atom labeling of β-CD.

In order to facilitate the descriptions that follow, we found it convenient to define a local system of coordinates. At each step of the simulation, the origin of the local system was located at the center of mass of the CD molecule, while the instantaneous unit vectors $\hat{x}'$, $\hat{y}'$, and $\hat{z}'$ were aligned parallel to the principal axes, according to the magnitude of the corresponding moments of inertia, that is, $I_{x'} < I_{y'} < I_{z'}$, and with the z' axis pointing toward the wider, secondary-hydroxyl rim of the CD (see Figure 2a).

Our experiments started with a molecular dynamics run in vacuo, during which C153 approached the wider rim of CD, previously equilibrated at $T = 100$ K. In this thermal range, thermal fluctuations are mild enough so as to preserve the overall geometrical arrangement corresponding to the global minimum configuration. Two orientations that differ in the alignment of the dipole moment of C153 relative to the z' axis, parallel and antiparallel, were tested. From an energetic point of view, the antiparallel encapsulation turned out to be more stable, and this was also the one where we found a larger extent of encapsulation of the probe. Consequently, we restricted our sampling to this initial mode of docking. The CD−C153 complex was then immersed in aqueous systems, previously equilibrated at $T = 298$ K. All water molecules that were found to overlap with those of the complex were removed. The systems were further equilibrated at relatively high temperature, $T = 700$ K, for additional periods of 200 ps in simulations runs, during which only water molecules were allowed to move. In doing so, we tried to eliminate eventual spurious effects arising from trapping in local potential energy basins. From then on, the systems were gradually cooled down to ambient conditions by multiple rescalings of the atomic velocities. During the final stages, we released constraints on the CD−C153 complex and the systems were allowed to equilibrate at room temperature for about 200 ps.

Two kinds of simulation experiments were performed. Equilibrium averages for DIMEB and TRIMEB in their S_0 and S_1 electronic states were collected along a series of five microcanonical simulation runs, each one lasting typically 1 ns. In addition, S_0 configurations separated by 20 ps intervals were

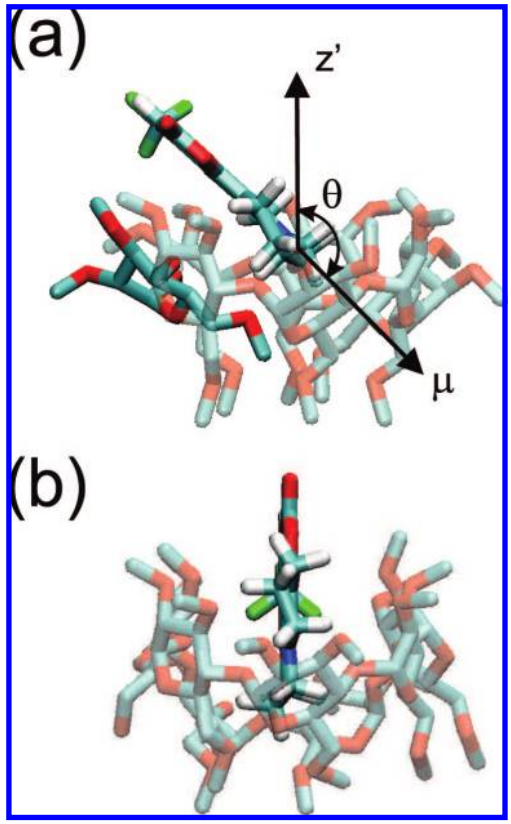

Figure 2. Typical configurations for coumarin 153−DIMEB complexes in aqueous solutions: (a) slanted geometry; (b) upright geometry. In panel a, the glucose unit lying closer to the probe is rendered in darker colors.

used as initial conditions of a second series of nonequilibrium experiments in which, at $t = 0$, the original charge distribution of the CD was changed to that corresponding to the S_1 state. From these initial configurations, we followed the relaxations of the systems for about 8 ps. In all simulations, long-range Coulomb interactions were treated by a particle mesh procedure[64] to compute Ewald sums.

III. Equilibrium Solvation Structures of CD−C153 Complexes

Before addressing the analysis of the dynamic characteristics of the solvation of coumarin−cyclodextrin complexes in aqueous solutions, we will briefly review some important aspects pertaining to the spatial and orientational correlations involving the different components of the system. Our structural description will be based on the analysis of probability distributions associated with a few relevant order parameters: the first one concerns the overall shape of the CD. In this context, a representative magnitude is the eccentricity of the ring defined as:

$$\epsilon = \left(1 - \frac{a^2}{b^2}\right)^{1/2} \tag{1}$$

where

$$a^2 = \frac{I_{z'} - (I_{y'} - I_{x'})}{2}$$
$$b^2 = \frac{I_{z'} + (I_{y'} - I_{x'})}{2} \tag{2}$$

Plots of the probability densities for ϵ corresponding to two substituted CD are shown in Figure 3a. The overall shape of the distributions resembles a Gaussian profile, slightly stretched along the low ϵ branch, with mean values $\bar{\epsilon}_{\mathrm{DIMEB}} = 0.54 \pm 0.04$ and $\bar{\epsilon}_{\mathrm{TRIMEB}} = 0.50 \pm 0.06$. These values should be compared to the one recently reported by us for β-CD in water, $\bar{\epsilon}_{\mathrm{CD}} \sim 0.6$.[65] The lower eccentricity found here would suggest that the insertion of the fluorescent probe helps to preserve the circular geometry of the central ring that would be, otherwise, altered to a larger extent by solvent fluctuations. In addition, the lowest value for TRIMEB would reveal that these solvent effects also seem to become milder as the number of methylations increases.

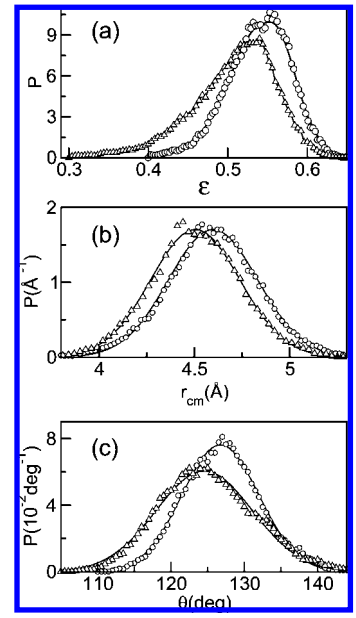

Figure 3. Probability distributions associated with different order parameters: (a) C153 eccentricity; (b) CD−C153 center of mass distance; (c) C153 tilt (see text). (○) DIMEB and (△) TRIMEB results are shown.

We now turn to the analysis of spatial correlations between CD and C153. Fluctuations in $r_{\mathrm{cm}} = |r_{\mathrm{cm}}^{\mathrm{CD}} - r_{\mathrm{cm}}^{\mathrm{C153}}|$, the distance between the centers of mass of the two molecules, may prove adequate to quantify the degree of confinement. In Figure 3b we present results for the probability distributions associated with r_{cm}. At first glance, the profiles also look Gaussian, with average values $\bar{r} = 4.6 \pm 0.2$ Å for DIMEB and $\bar{r} = 4.5 \pm 0.2$ Å for TRIMEB. We remark that the small magnitudes of the latter variances reveal that the C153 remains tightly trapped within the central cavities of both cyclodextrins and that the "in and out" dynamics of the probe involves modes with very small amplitudes.

Concerning orientational correlations, one observable of interest is the tilt angle, defined as

$$\cos\theta = \frac{\boldsymbol{\mu}\hat{\boldsymbol{z}}'}{|\boldsymbol{\mu}|} \tag{3}$$

The corresponding histograms for angle θ are shown in Figure 3c. The results indicate that the coumarin remains inserted within the cyclodextrin cavities with tilt angles close to $\bar{\theta} = 126° \pm 5°$ for DIMEB and $\bar{\theta} = 124° \pm 6°$ for TRIMEB. A snapshot of a typical configuration exhibiting such arrangement for the C153−DIMEB dimer is shown in Figure 2a. The direct inspection of the time evolution of $\theta(t)$ along the equilibrium trajectories that we performed (all initially prepared with $\theta \sim 180°$) showed that, in ~70% of them, the slanted geometrical arrangement is developed in the course of a few hundreds of

Downloaded by COMISION NAC DE ENERGIA ATOMICA CNEA on October 7, 2009 | http://pubs.acs.org
Publication Date (Web): July 2, 2008 | doi: 10.1021/jp8023765

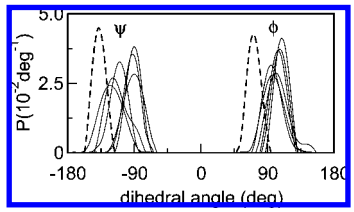

Figure 4. Probability distributions associated with the seven (1−4) linkages in DIMEB. The dashed lines corresponds to the distributions of two dihedral angles flanking the glucose unit that lies closer to the plane of the CD.

picoseconds. Moreover, we could also verify that the changes in orientation were preceded by important torsions of the angles ψ (C5−C4−O1′−C1′) and ϕ (C4−O1′−C1′−O5′), mostly localized at one glycosidic (1−4) linkage. These rotations, in turn, facilitate the approach of the coumarin to one tagged glucose unit, in such a way that both moieties may remain with their planes parallel over time periods lasting several hundreds of picoseconds (see Figure 2a). In Figure 4, we show the probability distributions corresponding to the seven ψ and ϕ angles of the DIMEB molecule, obtained from a 1 ns trajectory. In both sets of results, one distribution (drawn with thick, dashed lines) is clearly distinguished from the rest, due to its shifted profile ($\bar{\psi} = -138°$ and $\bar{\phi} = 71°$) and also to its somewhat narrower width. Subsequent analysis showed that these angles corresponded to the ones flanking the glucose unit which lies closest to the coumarin.

Before closing this section, we point out that the particular CD−C153 geometrical arrangement we have just presented in the previous paragraphs prevents the confinement of additional water molecules within the central cavity. It is well-established that, in the absence of guests, a β-CD can allocate typically ∼5−7 water molecules in its central cavity.[41,42,65,66] Taking into account the cavity size (a cylindrical volume of radius ∼5 Å and height ∼7 Å) and the linear dimensions of the C153 molecule, one can safely invoke steric restrictions to explain the absence of solvent in the interior of the CD.

IV. Rotational Dynamics

We will start our dynamic analysis by examining rotational motions of confined probes. In order to make contact with information obtained from time-dependent fluorescent depolarization experiments,[67] we will consider equilibrium time correlation functions of the type

$$C_\mu(t) = \langle P_2[\cos\theta_\mu(t)]\rangle \tag{4}$$

where

$$\cos\theta_\mu(t) = \frac{\boldsymbol{\mu}(t)\cdot\boldsymbol{\mu}(0)}{|\boldsymbol{\mu}|^2} \tag{5}$$

In the previous equations, $P_2(x) = {}^1/_2(3x^2 - 1)$ represents the second Legendre polynomial and broken brackets denote an equilibrium ensemble average. Results for the decay of $C_\mu(t)$ along a 20 ps time interval are presented in the top panel of Figure 5. After ∼1 ps initial transient, the curves present smooth decays that can be reasonably well described by single exponentials, with practically the same characteristic time scale, $\tau_\mu \sim 260$ ps.

It is also of interest to compare these decays to those describing the overall tumbling dynamics of the CD molecule. To do so, we considered correlation functions involving the angle subtended by unit vectors along the z' directions as time progresses, namely:

$$C_{z'}(t) = \langle P_2[\cos\theta_{z'}(t)]\rangle \tag{6}$$

with

$$\cos\theta_{z'}(t) = \mathbf{z}'(t)\cdot\hat{\mathbf{z}}'(0) \tag{7}$$

Results for the decays of $C_{z'}(t)$ are also shown in the same panel of Figure 5. Except for the magnitude of the initial decays–which, for $C_{z'}$, look somewhat smaller–the orders of magnitude of the characteristic time scales describing the long time decays of this correlation function, $\tau_{z'} \sim 360$ ps, and τ_μ look similar. These observations agree with the tightly confined picture previously described and would suggest that the gross features of the rotational dynamics of the encapsulated C153 at long time spans are dictated to a large extent by that of the CD. Of course, the orientational decay of C153 is somewhat faster compared to that of CD, due to the additional relaxation channels available for the guest molecule, mainly involving motions within the CD cavity.

The geometrical restrictions imposed by the confinement upon the coumarin have clear implications on the time evolution of the orientation of the probe relative to the local CD frame. In the bottom panel of Figure 5 we present results for the decays of the second Legendre polynomial for cos θ (cf. eq 3). After a subpicosecond librational transient, the two curves smoothly decay toward apparent plateau values.

To rationalize these observations, we will resort to the classical "wobbling-in-a-cone" rotational diffusion model.[68–70] At its simplest version, two parameters are involved in the model: a wobbling diffusion time scale τ_w, proportional to the inverse of the rotational diffusional constant, and the azimuthal angle θ_0, which gauges the extent of orientational constraint for the probe. The resulting expression for $C(t)$ is

$$C(t) = A_\infty + (1 - A_\infty)e^{-t/\tau_w} \tag{8}$$

where the constant A_∞ represents the asymptotic plateau value of the correlation function at long time intervals. Assuming a random distribution of orientations, A_∞ is related to θ_0:

$$A_\infty = \left[\frac{1}{2}\cos\theta_0(1 + \cos\theta_0)\right]^2 \tag{9}$$

The results displayed in Figure 3c clearly show that the distributions for cos θ for the trapped C153 do not look uniform within a conical volume. However, one can still exploit the

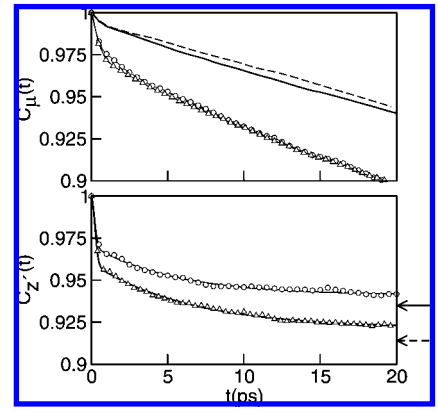

Figure 5. Time correlation functions for orientational correlations (see text). Top panel: $C_\mu(t)$ for C153 encapsulated in (○) DIMEB and (△) TRIMEB. Also shown are results for $C_{z'}$: (—) DIMEB and (---) TRIMEB. Bottom panel: same as the top panel for the orientational decorrelation of cos θ. Lines represent nonlinear fits of the simulation results; arrows indicate estimates for A_∞ from eq 9. Same labeling as in the top panel.

Downloaded by COMISION NAC DE ENERGIA ATOMICA CNEA on October 7, 2009 | http://pubs.acs.org
Publication Date (Web): July 2, 2008 | doi: 10.1021/jp8023765

simplicity of the "wobbling-in-a-cone" model to bring additional consistency to our results. To do so, we have used the variances $\Delta\cos\theta$ obtained from our simulation results to compute values of $\cos\theta_0$ for "*effective*" uniform distributions of orientations, namely:

$$\Delta\cos\theta = \left[\frac{\cos^2\theta_0}{12} - \frac{\cos\theta_0}{6} + \frac{1}{12}\right]^{1/2} \quad (10)$$

From the data shown in Figure 3c, a direct change of variables yields $\Delta\cos\theta = 0.006$ ($\Delta\cos\theta = 0.009$) or, equivalently, $\cos\theta_0 = 0.979$ ($\cos\theta_0 = 0.970$) for DIMEB (TRIMEB). With the latter numbers and eq 9, we computed the model predicted plateau values $A_\infty = 0.938$ and $A_\infty = 0.913$ (see arrows on the right-hand side of the *y*- axis). On the other hand, a fit according to eq 8 of the postlibrational portion of the curves (shown with solid lines) yields $\tau_w = 0.45$ ps and $A_\infty = 0.942$ for DIMEB and $\tau_w = 0.49$ ps and $A_\infty = 0.924$ for TRIMEB. The very good agreement between the latter values and the fitted ones clearly brings support to the physical picture that portrays CD−C153 as a tightly bound complex, in which the probe and CD present similar rotational characteristics at long time spans.

V. Solvation Dynamics

Following a similar line of analysis, we will now examine the dynamical aspects associated with the solvation of confined probes. The relevant experimental information obtained from time-dependent Stokes shift spectroscopy involves the temporal evolution of $S(t)$:

$$S(t) = \frac{\nu(t) - \nu(\infty)}{\nu(0) - \nu(\infty)} \quad (11)$$

where $\nu(t)$ represents the position of the maximum of the emission band of the fluorescence at time t. In computer simulation studies, and within the Franck−Condon approximation, the time evolution of the latter quantity can be conveniently monitored by that of

$$S(t) = \frac{\langle \Delta E(t) - \Delta E(\infty)\rangle_{ne}}{\langle \Delta E(0) - \Delta E(\infty)\rangle_{ne}} \quad (12)$$

In the previous equation, broken brackets with subscript ne denote an average obtained from a set of trajectories with initial conditions taken from an ensemble of nonequilibrium configurations.[71] In addition, $\Delta E(t)$ represents the solvent contribution to the energy gap between the S_1 and S_0 Born−Oppenheimer potential energy surfaces at time t:

$$\Delta E = \sum_\alpha \Delta q_\alpha V_\alpha(t) \quad (13)$$

where Δq_α and $V_\alpha(t)$ represent the charge jump and the Coulombic potential at the α site of C153, respectively. Discrimination into contributions from water (W) and cyclodextrin (CD) gives rise to a decomposition of the total response into two contributions:

$$S(t) = c_W S_W + c_{CD} S_{CD} \quad (14)$$

with

$$c_i = \frac{\langle \Delta E_i(0) - \Delta E_i(\infty)\rangle_{ne}}{\langle \Delta E(0) - \Delta E(\infty)\rangle_{ne}} \quad (15)$$

and

$$S_i(t) = \frac{\langle \Delta E_i(t) - \Delta E_i(\infty)\rangle_{ne}}{\langle \Delta E_i(0) - \Delta E_i(\infty)\rangle_{ne}} \quad (16)$$

In eqs 14, 15, and 16, c_i represents the fractional contribution of the ith component (i = W or CD) to the total Stokes shift while $S_i(t)$ is the normalized response of component i to the charge jumps operated in C153. Here, $\Delta E_i(\infty)$ correspond to averages of $\Delta E_i(t)$ taken over the last 2 ps of the nonequilibrium dynamics.

Before we analyze the dynamic characteristics, it will be useful to briefly examine the magnitude of the relative weights of W and CD to the total energy gap provided by the environment. The results are displayed in Table 1 along with our estimates for the total Stokes shifts $\Delta\nu = \langle\Delta E(0) - \Delta E(\infty)\rangle$. As expected, contributions to the total shift from the whole set of water molecules are substantially larger (approximately a factor of 5−6) than the individual contribution from either CD molecule. Moreover, the absence of any relevant changes in the solvation structures with functionalization leads to a small ($\sim$150 cm $^{-1}$) modification of $\Delta\nu$. However, the overall agreement between these estimates and the experimental information available is not totally satisfactory: while our TRIMEB prediction is $\sim$20% lower, the DIMEB one overestimates the experimental result reported in ref 21 by a factor of $\sim$1.5. Discrepancies of similar magnitude have been reported for the case of C153 in aqueous solutions and also in polar mixtures.[46,48,49] However, and very likely due to a cancelation of errors, the dynamic predictions obtained from this type of calculations normally remain quite accurate when compared to direct experimental information.[46,48] Moreover, these average values are likely to be affected by an additional uncertainty, originated in our choice of $\Delta E(\infty)$. For the purposes of clarity, we prefer to postpone the discussion of this issue to the forthcoming section.

In Figure 6 we present results for the water and CD contributions to the nonequilibrium response. The results correspond to a series of 200 relaxations initiated with the C153 lying in its slanted encapsulation. In the top panel, we present results for S_W. As a reference, and in order to identify possible effects originated from the encapsulation of the probe, we have also included results from simulation experiments of water relaxations of "free" C153, taken from Figure 2 of ref 48. One can see no major effects originated either in the encapsulation of the probe or in the particular functionalization considered. For both CD, the plots present the well-documented dual behavior[72] characterized by inertial branches in the subpicosecond time domain, which account for a substantial fraction of the total response (in the present case, on the order of $\sim$60%). These sharp decays are followed by much slower, diffusive relaxations, that can be reasonably well fitted by single exponentials with characteristic time $\tau_s = 1.2$ ps (DIMEB) and $\tau_s = 1.0$ ps (TRIMEB). The mechanisms operating during both stages are also well-established: while the first portion includes librational modes, the dynamics ascribed to the second stages involve mostly translational motions.

TABLE 1: Solvation Parameters for the Solvation of Trapped C153 within DIMEB and TRIMEB in Aqueous Solutions

cyclodextrin	c_W	c_{CD}	$\Delta\nu$ (cm^{-1})	$\Delta\nu^{exp}$
DIMEB	0.88	0.12	963	600 [a]
TRIMEB	0.84	0.16	807	1050 [a]

[a] From ref 21.

Downloaded by COMISION NAC DE ENERGIA ATOMICA CNEA on October 7, 2009 | http://pubs.acs.org
Publication Date (Web): July 2, 2008 | doi: 10.1021/jp8023765

Downloaded by COMISION NAC DE ENERGIA ATOMICA CNEA on October 7, 2009 | http://pubs.acs.org
Publication Date (Web): July 2, 2008 | doi: 10.1021/jp8023765

The nonequilibrium responses of CD are presented in the bottom panel of Figure 6. From a qualitative point of view, and compared to the water responses, the relaxations of DIMEB and TRIMEB are characterized by two distinctive features: (i) There is a sharp, inertial decay in the subpicosecond time regime and no subsequent diffusional branch. Gaussian fits of both $S_{CD}(t)$ curves yield practically identical decays: $\omega^{-1} \sim 85$ ps. The absence of the bimodal character reveals little changes in spatial and orientational correlations involving C153 and CD molecules following the excitation. This, in turn, would also explain why all our efforts to identify physically meaningful changes in relevant observables, such as r_{cm} or cos θ, were unsuccessful. As such, the only dynamic modes of the CD molecules able to respond to the electronic excitation of the C153 are small-amplitude, intramolecular motions that do not perturb the overall geometry of the encapsulation arrangement. (ii) A second distinctive feature is also evident: both CD relaxations look much noisier than those corresponding to water. We tend to believe that this feature is the result of the combined effects of a relatively small Stokes shift compared to the size of the typical spontaneous fluctuations ($\Delta\nu_{CD} \sim \langle(\delta\Delta E_{CD})^2\rangle^{1/2} \sim 200-300$ cm^{-1}), and large cancelation effects in the CD response, both affecting the quality of the statistics. To clarify the latter point, we found it useful to perform an equivalent decomposition to that shown in eq 14 for the total response, based on C153 sites contributions, namely[48]

$$S(t) = \sum_{\alpha} c_{\alpha} S_{\alpha}(t) \tag{17}$$

Now, the index α labels different coumarin sites. The new coefficients c_α represent the weights for the individual normalized site responses $S_\alpha(t)$. It has been previously reported that, for polyatomic probes, some site weights may exhibit negative signs.[48] In the present case, it is illustrative to examine contributions from sites that are deeply inserted in the CD, that is, those lying along the N4−C15 ring. For the latter sites, we found the following sequence: $c_{N4} = 0.20$, $c_{C5} = -0.12$, $c_{C6} = 0.08$, $c_{C7} = -0.15$, and $c_{C15} = 0.16$, which clearly correlates to that observed for the charge jump:[49] $\Delta q_{N4} = 0.11$e, $\Delta q_{C5} = -0.063$e, $\Delta q_{C6} = 0.046$e, $\Delta q_{C7} = -0.108$e, and $\Delta q_{C15} = 0.109$e. Negative values of c_α should be interpreted as dynamic modes of the environment evolving in the opposite direction to that predicted exclusively on the basis of the charge jump of the particular atom considered.[48] Here, they would also reveal that,

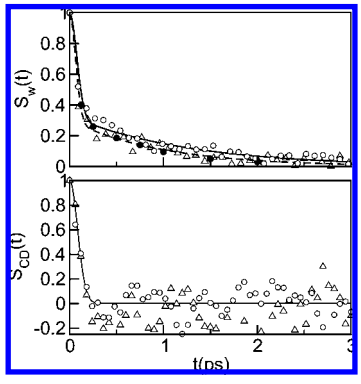

Figure 6. Contributions of (top) water and (bottom) CD to the solvation responses for encapsulated C153 in (○, –) DIMEB and (△, ---) TRIMEB in aqueous solutions. In the top panel, the lines represent single-exponential fits of the postlibrational portion of the responses; in the bottom panel, the solid line represents a Gaussian decay with $\omega^{-1} =$ 85 fs. Also shown are results for the water response of "free" C153, from ref 48 (●).

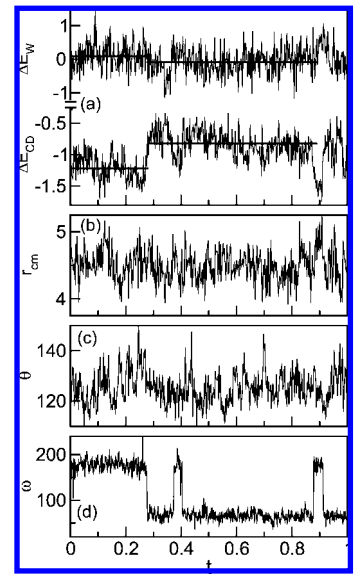

Figure 7. Time evolution of different observables for an equilibrium run for C153−TRIMEB complex: (a) Energy gaps (10^3 cm^{-1}); (b) r_{cm} (angstroms); (c) tilt angle (degrees); (d) C4−C5−C6−O6 dihedral angle (degrees); for the purposes of clarity, negative angles are shown shifted by 360°. The time is expressed in nanoseconds.

due to the constraints imposed by its partial rigidity, CD is unable to "respond" to all local changes operating in the charge distribution of C153 toward stable equilibrium. This situation is particularly evident in cases such as the present one, where sign alternations in the charge density prevail over length scales comparable to the size of a typical intramolecular bond, say 1−2 Å.

VI. Dynamics in the Nanosecond Time Domain

Direct inspection of the curves shown in Figure 6 shows that, within the error bars of our statistics, all relaxations seem to be accomplished after, say, the first 3 ps. As such, they do not provide perceptible signs of retardations of orientational or translational modes of the solvent, a feature that is normally invoked to rationalize the ultraslow decays of the experimental signals. As an alternative strategy to detect possible sources of ultraslow modes, we examined the characteristics of the time evolutions of several observables of interest along sufficiently long equilibrium runs.

In Figure 7a, we present results for $\Delta E_W(t)$ and $\Delta E_{CD}(t)$, the water and TRIMEB contributions to the energy gap, obtained from a typical, 1 ns trajectory with the probe in the S_0 electronic state. At first glance, it is clear that, at $t \sim 0.28$ ns, there is a sudden transition in the CD contribution to the energy gap that jumps from $\Delta E_{CD} \sim -1200$ cm^{-1} up to values close to $\Delta E_{CD} \sim -800$ cm^{-1}. Interestingly, a similar inspection of the time evolutions of the two relevant order parameters for the encapsulation, namely, r_{cm} and cos θ (Figure 7b,c), reveals that the sudden transition is neither preceded nor followed by clear changes in the geometry of the encapsulation arrangement. Instead, we did find a clear correspondence between the time evolution of ΔE_{CD} and those of the dihedral angles ω describing rotations along the primary hydroxyl bond sequences O5−C5−C6−O6 and C4−C5−C6−O6 of the glucose unit lying closest to the probe (see Figure 7d). In fact, we found that a sizable extent of the ∼400 cm^{-1} change in the energy gap arises from the individual contribution of the O6−N4 coupling. In order to make this point even more clear, in the sequence shown in Figure 8, one can see that the trans-to-gauche interconversion causes the "detachment" of the O6 atom from the N4.

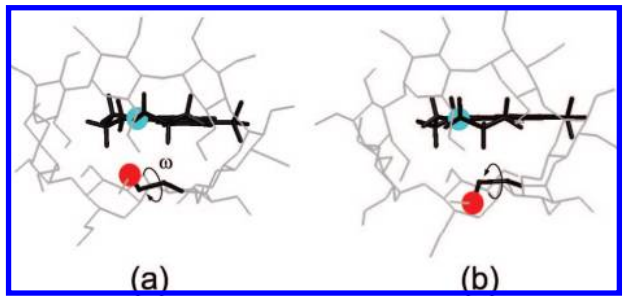

Figure 8. Isomerization along the primary hydroxyl chain of TRIMEB, viewed from the primary hydroxyl, narrower rim. The snapshots correspond to configurations taken from the trajectory shown in Figure 7, at (a) $t = 0.27$ ns and (b) $t = 0.29$ ns. For the purpose of clarity, the O4−C5−C6−O6 chain is rendered in dark colors while the O6 (TRIMEB) and N4 (C153) sites are shown as colored spheres.

Of course, the change in the geometrical arrangement of C153 is also reflected, although to a much milder degree, by changes in ΔE_W. As a reference, consider the horizontal lines drawn in Figure 7a, which represent average values taken during the first 0.28 ns and the subsequent 0.6 ns (for the purposes of the present discussion, the brief recrossing episode at $t \sim 0.4$ ns was disregarded). One can clearly see that the relative effects of the observed changes are much more pronounced in the CD contribution than in the solvent one, where the jump in ΔE_W is $\sim\Delta E_{CD}/2$. We also point out that these qualitative features were also found in equilibrium runs for TRIMEB-encapsulated C153, regardless of the particular electronic-state charge configuration considered.

Several important conclusions can be drawn from the previous scenario: (i) first, the gauche−trans interconversion operated by the rotation of the relevant primary hydroxyl chain may affect the overall response of the environment in a sensible fashion; (ii) the interconversions also modify, although to a much lesser extent, the solvent contributions to the total energy gap; (iii) the latter modifications do not seem to originate in slow motions of the water molecules but they rather correspond to a response to the geometrical change; (iv) the dynamics of the interconversion processes involve characteristic time scales τ_{int} on the order of several hundreds of picoseconds, a time span which is comparable to the total length of our simulation experiments. The magnitude of this time scale clearly precludes an accurate calculation of $\langle\Delta E(\infty)\rangle_{ne}$ in the usual fashion, via $\langle\Delta E\rangle_{S_1}$ which, otherwise, would require prohibitively long trajectories. This justifies the ad hoc criterion that we adopted for the choice of $\langle\Delta E(\infty)\rangle_{ne}$ in eqs 12, 15, and 16).

Before closing this section, we comment on a second slow process that may also affect the dynamics of solvation of C153. We are referring to overall modifications of the probe tilt. In the course of several trajectories we found the persistence of upright geometries, that is, $\cos\theta \sim 1$ (see Figure 2b) over time periods of several hundreds of picoseconds. Successive interconversions between slanted and upright configurations were found to be much more rare events, and we were unable to obtain a clear assessment of their relative importance. Moreover, their implications in the magnitude of the resulting energy gap were much less noticeable than in the previous case, most likely due to canceling effects. Anyhow, as such, they should also be considered in much more comprehensive analyses involving dynamics in the nanosecond time domain, a temporal realm that is certainly well beyond the scope of this study.

VII. Concluding Remarks

The results presented in this paper describe new insights related to equilibrium and dynamic characteristics of the solvation of midsize fluorescent probes within hydrophobic cavities of β-cyclodextrins. The first important conclusion that can be extracted from our simulation results concerns the tight nature of the confinement provided by both cyclodextrins. This unusual stability seems to be articulated by the preferential solvation of C153 by one particular glucose unit, in an overall slanted arrangement. Moreover, this geometry does not seem to be affected, either permanently or transiently, by vertical electronic excitations of the probe. This observation is in accord with previous analyses in which host−coumarin dispersion (non-Coulombic) interactions were identified as the controlling agents of the prevailing confinement within cyclodextrin cavities.[73] In a related context, a similar stable solvation geometry of the fluorescent probe has also been suggested in previous simulations experiments of C460 in γ-CD, although in the latter case, the stabilization would operate via hydrogen bonds involving the coumarin carbonyl oxygen and primary hydroxyl groups. Of course, there are other geometric characteristics that contribute to the robustness of the CD−C153 complex; perhaps the most important in the present case concerns an appropriate match between the length scales describing the size of the hydrophobic hollow of β-CD and the linear dimensions of a C153 molecule.

The second important observation is related to our rotational dynamics results that reveal very low sensitivity of the overall short-time dynamic behaviors with the degree of functionalization of the CD ring. DIMEB and TRIMEB relaxations present initial decays in the picosecond time domain that reflect fast, diffusional rotations within a tightly confined environment. These decays are followed by much slower relaxations with characteristic time $\tau_\mu \sim 260$ ps. Note that this time scale is much longer than the one reported for "free" C153 in water[27] (~100 ps) and comparable to the correlation time for nonfunctionalized β-CD in aqueous solutions:[11] 200−300 ps. Moreover, the rotational characteristics described here are in accord with those reported for confined resorfin and oxazine-188 in β-CD, two dyes with molecular sizes comparable to that of C153, and whose slow dynamic decays can be described by characteristic time scales on the order of ~300 ps (see Table 2 of ref 18). More importantly, our simulation results seem to be complementary to the experimental information reported in ref 21, where the shortest characteristic time scales detected in the fluorescence anisotropy decays were on the order of ~1 ns.

In accordance with the previous description, the solvation dynamics in the picosecond time domain does not show any major effects arising from the extent of functionalization either. Moreover, the water response, which accounts for approximately $^2/_3$ of the total relaxation, does nor differ substantially from that observed in the absence of encapsulation. Characteristic time scales for water contribution to the decay of the energy gap were found to be on the order of 1 ps and are smaller than even the fastest relaxation time scales reported in Table 3 of ref 21, $\tau_1 = 2.4$ ps (DIMEB) and $\tau_1 = 10.3$ ps (TRIMEB). On first consideration, and when the retardation that prevails in the dynamic modes of water molecules constrained in environments with restrictive geometries is taken into account, the latter observation may look quite unexpected. As a possible physical interpretation to account for these nonintuitive results, we can speculate on the combined effects of the following factors: (i) There are no water molecules trapped within the central hydrophobic cavity of the CD. We remark that, as a consequence of the tight fit of the probe, no water molecules were found to be actually confined in the central cavity of the CD. The present case represents perhaps a singular situation, and we tend to

Downloaded by COMISION NAC DE ENERGIA ATOMICA CNEA on October 7, 2009 | http://pubs.acs.org
Publication Date (Web): July 2, 2008 | doi: 10.1021/jp8023765

Downloaded by COMISION NAC DE ENERGIA ATOMICA CNEA on October 7, 2009 | http://pubs.acs.org
Publication Date (Web): July 2, 2008 | doi: 10.1021/jp8023765

believe that a similar solvation analysis performed on larger oligosaccharides (for example, γ-CD) and/or with smaller dyes would yield more clear signs of slow motions of trapped water. (ii) Also connected with this last point, note that the presence of the CD partially "tempers" the water response. In this way, the overall contribution from the solvent surrounding the CD−C153 complex would be comparable to that arising from second or more distant solvation shells, in similar excitation experiments involving a nonencapsulated dye. These solvent modes, in turn, should become necessarily softer, precluding a clear identification of eventual slower motions originated in limited diffusive or rotational motions. (iii) The consideration of di- and permethylated CD is also likely to introduce additional problems for the detection of slow motions. Given the more weakened nature of the hydrogen-bond network prevailing in the neighborhood of CD, dynamic effects arising from the confinement should become even more subtle. We finally remark that the slightly faster solvation response observed for TRIMEB agrees with recent interpretations of the experimental trends of dielectric relaxations, in terms of water exchange rates in the closest solvation shells of several functionalized CD.[45]

Concerning the CD temporal response, the relaxation is characterized by a single decay that, for all practical purposes, vanishes beyond the first picosecond. Given the strong rigidity of the molecule, the only modes that can respond in that time interval are fast, stiff intramolecular modes. In addition, the statistical quality of the recorded responses was significantly affected by canceling effects arising from different site contributions that exhibit alternating signs.

A final key aspect of the present work concerns an exploratory analysis that we performed along several equilibrium runs, looking for clues that would help us rationalize the persistence of Stokes shifts in the nanosecond time domain. In doing so, we found two possible sources of slow dynamics: (i) The first one involves the well-documented gauche−trans interconversion in the primary hydroxyl chain of the glucose unit that lies closer to the fluorescent probe.[44] These interconversions involve a series of detachment-approaching episodes between the O6 site in the C153 and the nearby N4 site in the coumarin that are translated into important modifications of the coumarin energy gap contributions. These changes, in turn, are also accompanied by much milder modifications in the water contributions to the energy gap as well. (ii) The second source involves a much rarer overall change in the encapsulation arrangement, during which the slanted geometry of the CD−C153 complex turns into an upright, more symmetrical arrangement and vice versa. Given the limited number of episodes that we registered, the effects of these dynamic interconversions on the observed energy gaps were difficult to interpret.

A plausible scenario that emerges from these dynamic considerations would contemplate that the long time component of the experimental Stokes shifts should also reflect intramolecular motions in the CD, in addition to eventual slow dynamic modes of the solvent that we were unable to detect from our simulation results. More importantly, should this description remain correct, in the course of a typical fluorescence experiment, the recorded shifts would, at least, indicate two independent relaxation processes of the solvent: the first one, in the picosecond time domain, involving the response to the original electronic excitation of the probe and a second one, much more subtle, following subsequent gauche−trans interconversions along much longer time intervals. To the best of our knowledge, this new source of dynamics has never been contemplated in previous analyses and awaits more conclusive confirmations based on experimental and theoretical grounds as well.

Acknowledgment. J.R. and D.L. are staff members of CONICET–Argentina. We gratefully acknowledge financial support from the Direcció General de Recerca de la Generalitat de Catalunya (Grant 2005SGR-00779) and from the Ministerio de Educación y Ciencia of Spain (Grant FIS2006-12436-C02-01).

References and Notes

(1) For comprehensive information about cyclodextrins, see the special issue *Chem. Rev.* **1998**, *98*.
(2) Kano, K.; Kato, Y.; Kodera, N. *J. Chem. Soc., Perkin Trans.* **1996**, *2*, 1211.
(3) (a) Kuwabara, T.; Shiba, K.; Ozawa, M.; Miyajima, N.; Yasutada, S. *Tetrahedron Lett.* **2006**, *47*, 4433. (b) Clark, J. L.; Peinado, J.; Stezowski, J. J.; Vold, R. L.; Huang, Y.; Hoatson, G. L. *J. Phys. Chem. B* **2006**, *110*, 26375. (c) Menuel, S.; Duval, R. E.; Cuc, D.; Mutzenhardt, P.; Marsura, A. *New J. Chem.* **2007**, *31*, 995.
(4) Bhattacharyya, K. *Acc. Chem. Res.* **2003**, *36*, 95.
(5) Sen, P.; Roy, D.; Mondal, S. K.; Sahu, K.; Ghosh, S.; Bhattacharyya, K. *J. Phys. Chem. A* **2005**, *109*, 9716.
(6) Douhal, A.; Fiebig, T.; Chachisvilis, M.; Zewail, A. H. *J. Phys. Chem. A* **1998**, *102*, 1657.
(7) Douhal, A. *Chem. Rev.* **2004**, *104*, 1955.
(8) Douhal, A. *J. Photochem. Photobiol., A* **2005**, *173*, 229.
(9) Reija, B.; Al-Soufi, W.; Novo, M.; Tato, J. V. *J. Phys. Chem. B* **2005**, *109*, 1364.
(10) Okazaki, M.; Kuwata, K. *J. Phys. Chem.* **1984**, *88*, 4181.
(11) Uccello-Barretta, G.; Chiavacci, C.; Bertucci, C.; Salvadori, P. *Carbohydr. Res.* **1993**, *243*, 1.
(12) Behr, J. P.; Lehn, J. M. *J. Am. Chem. Soc.* **1976**, *98*, 1743.
(13) Pistolis, G.; Balomenou, I. *J. Phys. Chem. B* **2006**, *110*, 16428.
(14) Singh, M. K.; Pal, H.; Koti, A. S. R.; Sapre, A. V. *J. Phys. Chem. A* **2004**, *108*, 1465.
(15) El-Kemary, M.; Organero, J. A.; Santos, L.; Douhal, A. *J. Phys. Chem. B* **2006**, *110*, 14128.
(16) Sen, S.; Sukul, D.; Dutta, P.; Bhattacharyya, K. *J. Phys. Chem. A* **2001**, *105*, 10635.
(17) Vajda, S.; Jimenez, R.; Rosenthal, S. J.; Fidlert, V.; Fleming, G. R.; Castner, E. Q., Jr *J. Chem. Soc., Faraday. Trans* **1995**, *91*, 867.
(18) Balabai, N.; Linton, B.; Napper, A.; Priyadarshy, S.; Sukharevsky, A. P.; Waldeck, D. H. *J. Phys. Chem. B* **1998**, *102*, 9617.
(19) Roy, D.; Mondal, J.; Sahu, K.; Ghosh, S.; Sen, P.; Bhattacharyya, K. *J. Phys. Chem. A* **2005**, *109*, 7359.
(20) Das, P.; Chakrabarty, A.; Haldar, B.; Mallick, A.; Chattopadhyay, N. *J. Chem. Phys. B* **2007**, *111*, 7401.
(21) Sen, P.; Roy, D.; Mondal, S. K.; Sahu, K.; Ghosh, S.; Bhattacharyya, K. *J. Phys. Chem. A* **2005**, *109*, 9716.
(22) Harzeba, W.; Walker, G. C.; Johnson, A. E.; Barbara, P. F. *Chem. Phys.* **1991**, *152*, 57.
(23) (a) Horng, M.-L.; Gardecki, J. A.; Papazyan, A.; Maroncelli, M. *J. Phys. Chem.* **1995**, *99*, 17311. (b) Horng, M.-L.; Gardecki, J. A.; Maroncelli, M. *J. Phys. Chem. A* **1997**, *101*, 1030.
(24) (a) Chakrabarty, D.; Chakraborty, A.; Seth, D.; Hazra, P.; Sarkar, N. *Chem. Phys. Lett.* **2005**, *412*, 255. (b) Harza, P.; Chakraborty, D.; Sarkar, N. *Chem. Phys. Lett.* **2003**, *371*, 553.
(25) Chakrabarty, D.; Chakraborty, A.; Seth, D.; Hazra, P.; Sarkar, N. *Chem. Phys. Lett.* **2004**, *397*, 469.
(26) Jin, H.; Baker, G. A.; Arzhantsev, S.; Dong, J.; Maroncelli, M. *J. Phys. Chem.* **2007**, *111*, 7191, and references therein.
(27) Hazra, P.; Chakrabarty, D.; Chakraborty, A.; Sarkar, N. *Biochem. Biophys. Res. Commun.* **2004**, *314*, 543.
(28) Kometani, N.; Hoshihara, Y.; Yonezawa, Y.; Kajimoto, O.; Hara, K.; Ito, N. *J. Phys. Chem. A* **2004**, *108*, 9479.
(29) Baumann, R.; Ferrante, C.; Kneuper, E.; Deeg, F.-W.; Bräuchle, C. *J. Phys. Chem. A* **2003**, *107*, 2422.
(30) Nandi, N.; Bagchi, B. *J. Phys. Chem.* **1996**, *100*, 13914.
(31) Nandi, N.; Bagchi, B. *J. Phys. Chem. A* **1997**, *101*, 10954.
(32) Pizzitutti, F.; Marchi, M.; Sterpone, F.; Rossky, P. J. *J. Phys. Chem. B.* **2007**, *111*, 7584.
(33) Bhattacharyya, K.; Bagchi, B. *J. Phys. Chem. A* **2000**, *104*, 10603.
(34) For a comprhensive review article on simulation studies of cyclodextrins, see Lipkowitz, K. B. *Chem. Rev* **1998**, *98*, 1829, and references therein.
(35) Yu, Y.; Chipot, C.; Cai, W.; Shao, X. *J. Phys. Chem. B* **2006**, *110*, 6372.
(36) Naidoo, K. J.; Chen, J. Y.-J.; Jansson, J. L. M.; Widmalm, G.; Maliniak, A. *J. Phys. Chem. B* **2004**, *108*, 4236.

(37) Manunza, B.; Deiana, S.; Pintore, M.; Gessab, C. *J. Mol. Struct. (THEOCHEM)* **1997**, *419*, 133.
(38) Starikov, E. V.; Bräsicke, K.; Knapp, E. W.; Saenger, W. *Chem. Phys. Lett.* **2001**, *336*, 504.
(39) (a) Koehler, J. R. H.; Saenger, W.; van Gunsteren, W. F. *Eur. Biophys. J.* **1988**, *16*, 153. (b) Koehler, J. R. H.; Saenger, W.; van Gunsteren, W. F. *J. Mol. Biol.* **1988**, *203*, 241.
(40) Varady, J.; Wu, X.; Wang, S. *J. Phys. Chem. B* **2002**, *106*, 4863.
(41) Heine, T.; Dos Santos, H. F.; Patchkovski, S.; Duarte, H. A. *J. Phys. Chem. A* **2007**, *111*, 5648.
(42) Raffaini, G.; Ganazzoli, F. *Chem. Phys.* **2007**, *333*, 128.
(43) Oana, M.; Tintaru, A.; Gavriliu, D.; Maior, O.; Hillebrand, M. *J. Phys. Chem. B* **2002**, *106*, 257.
(44) See, for example, Engelsen, S. B.; Hervédu Penhoat, C.; Pérez, S. *J. Phys. Chem.* **1995**, *99*, 13334.
(45) Shikata, T.; Takahashi, R.; Satokawa, Y. *J. Phys. Chem. B.* **2007**, *111*, 12239.
(46) Kumar, P. V.; Maroncelli, M. *J. Chem. Phys.* **1995**, *103*, 3038.
(47) Baumann, R.; Ferrante, C.; Kneuper, E.; Deeg, F.-W.; Bräuchle, C. *J. Phys. Chem. A* **2003**, *107*, 2422.
(48) Martins, L.; Tamashiro, A.; Laria, D.; Skaf, M. S. *J. Chem. Phys.* **2003**, *118*, 5955.
(49) Martins, L.; Skaf, M. *Chem. Phys. Lett.* **2003**, *370*, 683.
(50) Cichos, F.; Brown, R.; Rempel, U.; von Borzyskowski, C. *J. Phys. Chem. A* **1999**, *103*, 2506.
(51) (a) Re, M.; Laria, D. *J. Phys. Chem.* **1997**, *101*, 10494. (b) Tamashiro, A.; Rodriguez, J.; Laria, D. *J. Phys. Chem. A* **2002**, *106*, 215.
(52) (a) Day, T. J. F.; Patey, G. N. *J. Chem. Phys.* **1999**, *110*, 10937. (b) Laria, D.; Skaf, M. S. *J. Chem. Phys.* **1999**, *111*, 300.
(53) Fonseca, T.; Ladanyi, B. *J. Phys. Chem.* **1991**, *95*, 2116.
(54) Ladanyi, B.; Maroncelli, M. *J. Chem. Phys.* **1998**, *109*, 3204.
(55) Thompson, W. H. *J. Chem. Phys.* **2002**, *117*, 6618.
(56) (a) Thompson, W. H. *J. Chem. Phys.* **2004**, *120*, 8125. (b) Gomez, J. A.; Thompson, W. H. *J. Chem. Phys. B* **2004**, *108*, 20144.
(57) (a) Berendsen, H. J. C.; Postma, J. P. M.; van Gunsteren, W. F.; Hermans, J. In *Intermolecular Forces*; Pullman, B., Ed.; Reidel: Dordrecht, The Netherlands, 1981; p 331. (b) Berweger, C. D.; van Gunsteren, W. F.; Müller-Plathe, F. *Chem. Phys. Lett.* **1995**, *232*, 429.
(58) (a) Moylan, C. R. *J. Phys. Chem.* **1994**, *98*, 13513. (b) Baumann, W.; Nagy, Z. *Pure Appl. Chem.* **1993**, *65*, 1729.
(59) Atomic coordinates for β-CD can be found at http://xray.bmc.uu.se/hicup/BCD/.
(60) (a) Koehler, J. R. H.; Saenger, W.; van Gunsteren, W. F. *Eur. Biophys. J.* **1987**, *15*, 197. (b) Koehler, J. R. H.; Saenger, W.; van Gunsteren, W. F. *Eur. Biophys. J.* **1987**, *15*, 211.
(61) Lawtrakul, L.; Viernstein, H.; Wolschann, P. *Int. J. Pharm.* **2003**, *256*, 33.
(62) Yua, H.; Amannb, M,.; Hanssona, T.; Köhlerb, J.; Wichb, G.; van Gunsteren, W. F. *Carbohydr. Res.* **2004**, *339*, 1697.
(63) Luzhkov, V.; Åqvist, J. *J. Am. Chem. Soc.* **1998**, *120*, 6131.
(64) (a) Darden, T. A.; York, D. M.; Pedersen, L. G. *J. Chem. Phys.* **1993**, *98*, 10089. (b) Essmann, U.; Perera, L,.; Berkowitz, M. L.; Darden, T.; Lee, H.; Pedersen, L. G. *J. Chem. Phys.* **1995**, *103*, 8577.
(65) Rodriguez, J.; Rico, D. H.; Dommeniani, L.; Laria, D. *J. Phys. Chem. B.* **2008**, *112*, 7522–7529.
(66) Betzel, C.; Saenger, W.; Hingerty, B. E.; Brown, G. M. *J. Am. Chem. Soc.* **1974**, *96*, 3630.
(67) Fleming, G. R.; Morris, J. M.; Robinson, G. W. *Chem. Phys.* **1976**, *17*, 91.
(68) Lipari, G.; Szabo, A. *Biophys. J.* **1980**, *30*, 489.
(69) Schröder, G.; Alexiev, U.; Grubmüller, H. *Biophys. J.* **2005**, *89*, 3757.
(70) (a) Kinosita, K., Jr.; Kawato, S.; Ikegami, A. *Biophys. J.* **1977**, *20*, 289. (b) Kawato, S.; Kinosita, K., Jr *Biophys. J.* **1981**, *36*, 277.
(71) Chandler, D. In *Introduction to Modern Statistical Mechanics*; Oxford University Press: New York, 1987; Chapt. 8.
(72) For review articles on solvation dynamics, see for example (a) Maroncelli, M. *J. Mol. Liq.* **1993**, *57*, 1. (b) Barbara, P. F.; Jarzeba, W. *Adv. Photochem.* **1990**, *15*, 1. (c) Bagchi, B. *Annu. Rev. Phys. Chem.* **1989**, *40*, 115. (d) Hynes, J. T. In *Ultrafast Dynamics of Chemical Systems*; Simon, J. D., Ed.; Kluwer: Dordrecht, The Netherlands, 1994; p 345.
(73) Liu, L.; Guo, Q.-X. *J. Inclusion Phenom. Macrocyclic Chem.* **2002**, *42*, 1.

JP8023765

Downloaded by COMISION NAC DE ENERGIA ATOMICA CNEA on October 7, 2009 | http://pubs.acs.org
Publication Date (Web): July 2, 2008 | doi: 10.1021/jp8023765